Stodieck, O. A., Cooper, J. E., & Weaver, P. M. (2016). Interpretation of Bending/Torsion Coupling for Swept, Nonhomogenous Wings. Journal of Aircraft, 53(4), 892-899. DOI: 10.2514/1.C033186

On the Interpretation of Bending-Torsion Coupling for Swept, Non-Homogenous Wings

O. Stodieck [1], J. E. Cooper[2], P. M. Weaver[3]

Department of Aerospace Engineering, University of Bristol, Queens Building,

University Walk, Bristol BS8 1TR, U.K.

The wide range of conflicting definitions of the axis on a general swept, non-uniform, non-homogenous wing about which there is no bending / torsion coupling are reviewed. A generalization of these definitions is made, with an emphasis on whether deflections and loads on a local streamwise section or the entire wing are considered. Determining this axis enables a better understanding as to why various aeroelastic tailoring and adaptive stiffness solutions are effective for flutter suppression and gust loads suppression applications. It is demonstrated, using a flexibility matrix approach, that the loading case must be considered in order to be able to accurately determine the flexural axis of a typical wing structure. The methodology is demonstrated using three numerical models: a simple swept wing, an aluminum wing box, and a tow-steered, variable stiffness, composite plate wing. Finally, the sensitivity of the flexural axis is considered and it is shown that the global flexural axis is much more sensitive to modeling or measurement errors than the local flexural axis.

Nomenclature

b	=	vector in simultaneous linear equations
c	=	local streamwise wing section chord-length
f_{ij}	=	flexibility influence coefficients
k_x, k_y, k_{xy}	=	local laminate bending and twisting curvatures
$\underline{r}$	=	vector of vertical deflections r_i (in z-direction) at wing reference degrees of freedom

[1] Ph.D. Research Student – Industrial Case Award, AIAA Student Member
[2] Royal Academy of Engineering Airbus Sir George White Professor of Aerospace Engineering, AFAIAA
[3] Professor in Lightweight Structures, AIAA member

s = wing span

w'' = wing spanwise bending curvature

x_L = location of the flexural center or local flexural axis on a streamwise wing section

x_G = location of the global flexural axis on a streamwise wing section

x, y, z = orthogonal wing coordinate-system

A = square matrix in simultaneous linear equations

D_{ij} = classical laminate theory D-matrix terms

$E(X)$ = statistical mean

F = flexibility matrix

P, Q = streamwise wing section shear loads (in z-direction)

M_x, M_y, M_{xy} = local laminate bending and twisting moments per unit-length

M, T = applied spanwise bending moment and torsion

$\underline{R}$ = vector of applied vertical force R_i (in z-direction) at wing reference degrees of freedom

R_i = applied vertical force at ith degree of freedom

θ = streamwise wing section twist angle relative to the root

θ' = streamwise wing section twist rate with respect to distance along the beam

σ = standard deviation

μ = warping constraint constant

I. Introduction

Aeroelasticity[1,2] has had a significant effect upon aircraft performance and wing designs since the beginning of manned flight. As well as the catastrophic phenomena of flutter and divergence, the in-flight wing shape, control surface performance, gust and maneuver response, and a wide range of critical load cases all depend upon the static and dynamic aeroelastic characteristics of each airplane[2]. Much work is currently being devoted to green designs, where aeroelastic effects are used beneficially in order to achieve reduced weight, loads alleviation and more efficient wing shape throughout the flight envelope. Possible design approaches to achieve these goals are aeroelastic tailoring[3] and adaptive stiffness morphing structures[4].

The key phenomenon to understanding aeroelastic behavior is the coupling between bending and torsion deflections, and their combined interactions with the aerodynamic forces. Indeed, all aeroelastic textbooks e.g. Refs 1 and 2, stress that the greater the distance between the aerodynamic center and the structural axis about which the bending and torsion motions are uncoupled (usually referred to as the flexural or elastic axis), then the larger the static aeroelastic twist, or the lower the flutter or divergence airspeeds. However, most aeroelastic design is undertaken through the optimization of coupled computational structural (FE) and aerodynamic (CFD or panel) models, and therefore a lot of the understanding as to why particular optimized solutions are found for the application of aeroelastically tailored structures or morphing is lost.

Despite its importance, there is still a great deal of confusion as to the actual definition of the axis about which there is no bending / torsion coupling. Indeed, it is some 60 years since Tatham wrote an article[3] attempting to differentiate between the shear center, flexural center and flexural axis. If swept wings are modeled as simple beams then, unless the coupling effects due to sweep are included (typically, a swept-back wing twists nose-downwards when a load is applied upwards – a process referred to as wash-out) in the analysis, errors in the analysis occur.

In this work, a review of the conflicting definitions of a range of relevant terms is made. In particular, it is shown that for wings that are either swept, non-uniform or non-homogeneous, concepts such as the shear center are not relevant for understanding of aeroelastic deformations, and that as well as the full wing geometry, the specific loading cases must be considered in order to truly determine how, for instance, passive loads alleviation strategies can be understood. A unification of the terminology is suggested, and then a flexibility matrix based methodology for determining the flexural axis is demonstrated, initially on a simple system, and then on two more complex examples involving a swept wing box and a composite anisotropic plate wing. Finally, the effect of uncertainty in the process to determine the flexural axis is considered. The objective is not to develop an approach for reducing a 3D FEM model to a simple beam structure, but to demonstrate how a greater understanding of wing aeroelastic behavior, and how to improve it, can be obtained through consideration of the flexural axis position.

II. Review of Relevant Literature

An investigation of the literature shows that there has been a widespread difference in the terminology used to describe the wing axis about which there is no bending / torsion coupling. A summary of the different terms and definitions found in the literature is provided in Table 1.

Table 1. Relevant definitions in the literature

Term	Definition	Reference
Shear center	"the point in the cross-section through which shear loads produce no twisting"	Megson (1999)[6]; Young (2002)[7]
	"the point in the plane of the section at which a shear force can be applied to the section without producing a rate of twist of the section"	Niles (1954)[8]; Peery(1950)[9]; Bisplinghoff (1996)[1]
	"the point about which the resultant moment of the shear flows in the walls of the section due to bending alone (i.e. without torque) is zero"	Tatham (1951)[5]; Kuhn (1936)[10]; Fung (1993)[11]
	"the position where a shear force can be applied without causing twist at that section"	Weisshaar (1987)[3]
	"For beams with bending-twist coupling such as composite beams, one can modify the definition of shear center by considering only the twist caused by the shear forces and excluding the twist produced by bending moment through the bending-twist coupling"	Yu(2002)[12]
Flexural center	"the point on a wing section at which a load must be applied so as to produce zero twist of that section relative to the root"	Tatham (1951)[5]
	"For a slender, curved, cantilever beam, the flexural center of a cross-section is defined as a point in that section, at which a shear force can be applied without producing a rotation of that section in its own plane."	Fung (1993)[11]

Center of twist / Torsional Center	"a point in a cross-section that remains stationary when a torque is applied in that section. If the supporting constraint of the beam is perfectly rigid, the flexural center coincides with the center of twist"	Fung (1993)[11]
Elastic Center	"If the distance between the [shear center] and the torsional center is sufficiently small to be neglected for practical purposes, the average location of the two centers will hereinafter be called the "elastic center" of the section." "The elastic center is, in practice, calculated as the [shear center]"	Kuhn (1936)[10]
Reference Axis	"In conventional engineering beam models, the Reference Axis is usually chosen to be the shear center or 'elastic axis' "	Weisshaar (1987)[3]
Elastic axis	"the spanwise line along which loads must be applied in order to produce only bending and no torsion of the wing at any station along the span"	Kuhn (1936)[10]
	"Forces applied to the wing on this axis produce translation of all sections of the beam without rotations and torques produce pure twisting of all sections about this axis."	Bisplinghoff (1996)[1]
	"the locus of shear centers"	Fung (1993)[11]; Yu(2002)[12]
	"the locus of points at which a transverse force may be applied and cause only bending and no twist (about a specified axis) on the section on which the force is applied"	Weisshaar (1987)[3]
Flexural line	"For a given loading, a flexural line is defined as a curve on which that loading may be applied, so that there results no twist at any section of the beam. In general, different load distributions correspond to different flexural lines, and there exist load distributions that do not have a flexural line."	Fung (1993)[11]
Flexural axis	"A straight line through the flexural center perpendicular to the plane of symmetry (or [wing] root plane)."	Tatham (1951)[5]

It may be seen that some terms have conflicting definitions, or share a definition with different terms. Whilst the usage of these terms and definitions may be justified in the context from which they are quoted, these can lead to confusion and misuse in the general case, potentially causing modeling errors as well as misinterpretations of analysis results. This lack of clarity is particularly true regarding the 'shear center' and the 'flexural center', which often tend to be confused for historical reasons[5]. While these two points may coincide for simple straight constant section homogenous beams, this is not the case in general. Ambiguity between the shear center and flexural center definitions also frequently leads to confusion between the elastic axis and the flexural axis. It seems important at this point to repeat Tatham's request that 'until definite standardization is introduced these terms should always be defined clearly whenever they are used'.

Independent work on straight helicopter rotor blades has shown a blade-position dependency of shear center location for anisotropically laminated box-beams where the effects of bend/twist coupling on straight beams is somewhat analogous to the bend/twist coupling response of isotropic but swept wings. Indeed, Rehfield and Atilgan[13] state "there will be twisting even if shear forces are applied at the shear center. Therefore, use of the locus of shear centers (elastic center) as a reference axis does not simplify a coupled bending/torsion analysis"

In an attempt to unify these conflicting descriptions, the following definitions are used throughout the rest of this study:

- The ***shear center*** is the position on a 2D cross-section where there is zero rate of change of twist along the beam for a shear load applied to that cross-section and does not include bend twist coupling (i.e. the shear center is characteristic of a particular section alone).
- The ***elastic axis*** is the locus of ***shear centers*** along a wing.
- The ***reference axis*** is the locus of some geometric or otherwise characteristic position (e.g. mid-chord, locus of mass centroids) along a wing.
- The ***flexural center*** is the position of a shear load on a streamwise wing cross-section where there is zero twist on that cross-section relative to the wing root, but not necessarily zero twist elsewhere on the wing (i.e. the flexural center is characteristic of the wing at a particular section).

- The ***local flexural axis*** is the locus of ***flexural centers*** along the wing.
- The ***global flexural axis*** is the position of a distributed set of loads applied simultaneously along a wing that will result in zero twist along the entire wing (i.e. the global flexural axis is characteristic of the wing under a specific load case).

To illustrate the difference between the flexural center and shear center concepts some figures from Tatham[5] are reproduced in Figure 1 for a typical aft-swept wing . Two different point loads are applied, one at the flexural center of streamwise section AB (a) and the other at the shear center of beam section AC (b). It can be clearly seen the streamwise section twist angle is only zero when the shear load is applied at the flexural center, while the rate of twist with respect to length is only zero when the shear load is applied at the shear center.

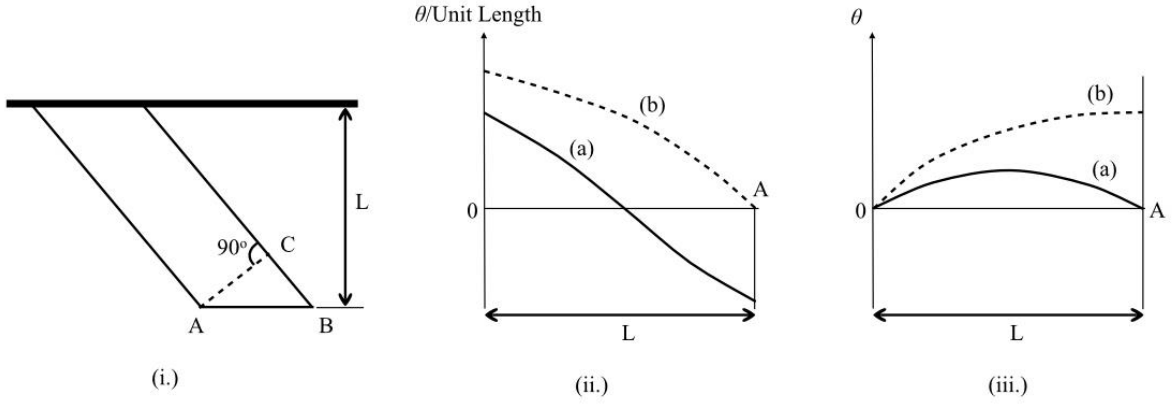

Figure 1. (i.) Aft-swept wing of span L with streamwise section AB and 2D-section AC; (ii.) hypothetical curves of twist per unit length for loads applied at (a) the flexural center and (b) the shear center at station A; (iii.) plot of total twist along the span, obtained as integrals of the curves in (ii.) (from Tatham[5])

Although the flexural axes locations are not required to calculate the static, dynamic and aeroelastic behavior of a wing, they are useful to understand its behavior from an aeroelastic point of view. By plotting the local and global flexural axes, we may gain some useful insight into the wing behavior for static and dynamic flight load cases which cannot be obtained by plotting the shear centers or elastic axis alone. In particular, the flexural axes may provide some physical insight into the workings of elastically tailored or morphing wing solutions which are generated using optimization methods.

The local flexural axis is a measure of the local bend-twist coupling along the wing span. The twist increment on a streamwise wing section induced by a shear force applied on that section can be qualitatively estimated by measuring the offset between the shear force line of action and the local flexural axis. For a given load distribution, the distance between the load application points and the global flexural axis is indicative of the twist induced along the wing span. The twist angle along the wing depends on the loading, the wing's torsional and bending stiffness distributions and also the inherent coupling between the two motions. For example, if the lift on a streamwise section acts aft of the flexural center then it generates a nose-down twist increment at this section, which tends to reduce the magnitude of the applied lift force at that section. Note that aft-swept wings exhibit an in-built bending torsion coupling (wash-out) whereby an upwards bending deflection results in a nose-down twist which typically provides a mechanism for alleviating gust loads and also contributes to the resulting increase in divergence airspeed. This coupling occurs due the flexural axis moving forward from the beam reference axis.

Determining the flexural axes enables a better understanding of how different aeroelastic solutions function in terms of bending – torsion coupling. Care must be taken when using beam structures instead of 3D FEM wing models (not the objective of this work) to ensure that correct bending-torsion couplings are included otherwise erroneous aeroelastic predictions will be obtained.

III. Determination of the Flexural Axes

In the following sections, a simple method based on the determination of the wing flexibility matrix is demonstrated that can be used to locate the local and global flexural axes. First, a very simple 2-strip wing model is considered to describe the equations used to determine the flexural axes and to show the importance of the load distribution on the location of the global flexural axis. Then, a more complex wing-box model and two composite wing models illustrate how geometrical features and material anisotropy affect the location of the flexural axes. Subsequent sensitivity analyses determine the effect of flexibility matrix errors on the location of the flexural axes. All analyses assume linear stiffness, small deflection behavior and no chordwise bending.

A. Use of the Flexibility Matrix to Determine the Flexural Axes of a Simple 2-Strip Wing Model

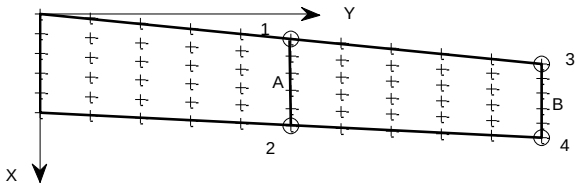

Figure 2. Simple 2-strip wing model

Consider the flat swept-wing type plate aluminum structure shown in Figure 2 with defined degrees of freedom (DOF) 1 – 4. The semi-span was 1m, thickness 0.5mm, with the root and tip chords 0.2m and 0.15m respectively, the local streamwise chords for sections A and B are defined as lengths c_A and c_B respectively. The wing was modelled using shell finite elements and unit vertical forces were applied independently to each of the DOF and the resulting deflections at all DOF were computed. The vertical deflections r_i obtained at each DOF i due to individual unit vertical loads R_i give each column of the flexibility matrix

$$\underline{\mathrm{R}} = \begin{bmatrix} r_1 \\ r_2 \\ r_3 \\ r_4 \end{bmatrix} = \begin{bmatrix} f_{11} & f_{12} & f_{13} & f_{14} \\ f_{21} & f_{22} & f_{23} & f_{24} \\ f_{31} & f_{32} & f_{33} & f_{34} \\ f_{41} & f_{42} & f_{43} & f_{44} \end{bmatrix} \begin{bmatrix} R_1 \\ R_2 \\ R_3 \\ R_4 \end{bmatrix} = \mathrm{F}\underline{\mathrm{R}}$$

$$\text{with } \mathrm{F} = \begin{bmatrix} 2.944 & 2.719 & 7.219 & 7.015 \\ 2.719 & 3.149 & 7.252 & 7.635 \\ 7.219 & 7.252 & 24.17 & 23.99 \\ 7.015 & 7.635 & 23.99 & 24.968 \end{bmatrix} * 1.e-4 \qquad (1)$$

where f_{ij} are the flexibility coefficients which are the displacement resulting at DOF i due to a unit load applied at DOF j. This flexibility matrix illustrate the typical characteristic of a swept back wing where washout, a nose-down twist coupling with upwards bending, occurs.

For a load P applied at some position x on a stream-wise section of chord c, it is necessary to find the equivalent loads at the leading and trailing edges on that section in order to apply a flexibility matrix type approach. From Figure 3, it can be seen that the equivalent load and moment for a stream-wise section of chord c, assuming that there is no chord-wise deflection and also that the zero angle of attack quarter chord pitching moment coefficient $C_{M0} = 0$, are obtained for leading and trailing edge forces R_1 and R_2 such that

$$P = R_1 + R_2 \;\; ; \;\; cR_2 = Px \qquad \Rightarrow R_1 = P(1 - \tfrac{x}{c}) \text{ and } R_2 = P\tfrac{x}{c} \tag{2}$$

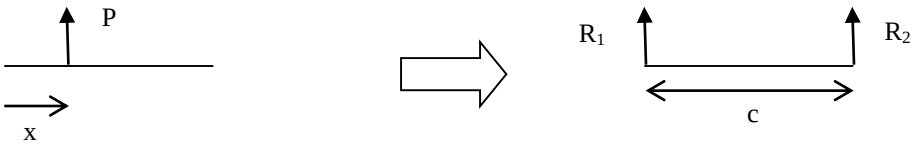

Figure 3. Determination of equivalent forces at the leading and trailing edge DOFs

The local flexural axis position at section A can be determined by applying a unit load at distance x_{FA} , which produces zero twist on that section. Making use of equation (2) we obtain the conditions

$$r_1 = r_2 \qquad R_1 = P(1 - \tfrac{x_{FA}}{c_A}) \qquad R_2 = P\tfrac{x_{FA}}{c_A} \qquad R_3 = 0 \qquad R_4 = 0 \tag{3}$$

and substitution into the top two rows of equation (1) gives the local flexural axis position at section A. A similar process can be repeated for streamwise section B using the bottom two rows. The resulting local flexural axis positions for each strip are found as

$$x_{FA} = \frac{c_A(f_{11} - f_{21})}{(f_{11} - f_{12} - f_{21} + f_{22})} \qquad \text{and} \qquad x_{FB} = \frac{c_B(f_{33} - f_{43})}{(f_{33} - f_{34} - f_{43} + f_{44})} \tag{4}$$

where the normalized flexural center location is measured from the leading edge (x=0) towards the trailing edge (x=1). For the given flexibility matrix in equation (1), this gives the two local flexural center positions as

$$\frac{x_{FA}}{c_A} = 0.3435 \qquad \text{and} \qquad \frac{x_{FB}}{c_B} = 0.1515 \tag{5}$$

which means that the flexural center position for strip A is over twice the distance from the leading edge as that for strip B.

The approach can be extended in order to find the global flexural axis positions x_{GA} and x_{GB} at sections A and B for a constant spanwise load. In this case, vertical loads P and Q are now applied simultaneously to both streamwise strips, such that there is zero twist in both of the strip, implying that the deflections at each degree of freedom are constrained such that $r_1 = r_2$ and $r_3 = r_4$, and the loads are defined by equation (2) for each strip. For the normalized (divide by each local chord) values of x_{GA} and x_{GB}, these constraints infer that equation (1) becomes

$$\underline{r} = \begin{bmatrix} r_1 \\ r_1 \\ r_3 \\ r_3 \end{bmatrix} = \begin{bmatrix} f_{11} & f_{12} & f_{13} & f_{14} \\ f_{21} & f_{22} & f_{23} & f_{24} \\ f_{31} & f_{32} & f_{33} & f_{34} \\ f_{41} & f_{42} & f_{43} & f_{44} \end{bmatrix} \begin{bmatrix} R_1 \\ R_2 \\ R_3 \\ R_4 \end{bmatrix} = \begin{bmatrix} f_{11} & f_{12} & f_{13} & f_{14} \\ f_{21} & f_{22} & f_{23} & f_{24} \\ f_{31} & f_{32} & f_{33} & f_{34} \\ f_{41} & f_{42} & f_{43} & f_{44} \end{bmatrix} \begin{bmatrix} P(1-x_{GA}) \\ Px_{GA} \\ Q(1-x_{GB}) \\ Qx_{GB} \end{bmatrix} \tag{6}$$

where there are now four unknowns, the positions of the applied loads and the bending deflections of each strip. Following some algebraic manipulation and elimination of the bending deflections, the global flexural axis positions are found from the set of simultaneous equations

$$\begin{bmatrix} P(f_{11}-f_{12}-f_{21}+f_{22}) & Q(f_{13}-f_{14}-f_{23}+f_{24}) \\ P(f_{31}-f_{32}-f_{41}+f_{42}) & Q(f_{33}-f_{34}-f_{43}+f_{44}) \end{bmatrix} \begin{bmatrix} x_{GA} \\ x_{GB} \end{bmatrix} = \begin{bmatrix} P(f_{11}-f_{12})+Q(f_{13}-f_{23}) \\ P(f_{31}-f_{41})+Q(f_{33}-f_{43}) \end{bmatrix} \tag{7}$$

which, for the given flexibility matrix, and assuming unit loads P = Q gives

$$\frac{x_{GA}}{c_A} = -0.0050 \qquad \text{and} \qquad \frac{x_{GB}}{c_B} = 0.3327 \tag{8}$$

It can be seen that these values are significantly different from the local flexural axis values found previously, and that the global flexural axis on strip A is now slightly upstream of the leading edge.

The global flexural axis positions depend upon the ratio between the loads on strips A and B. Figure 4 shows the change of position of the global flexural axis position with respect to the ratio of load B / load A and which is load-ratio dependent; its position on strip A varies a great deal, always being forward of the leading edge for loads ratios > 1 whereas that of strip B lies around the 35% chord position for all cases. Figure 5 shows the different positions of the shear center, local and global flexural axes for unit loading, double in-board load, and double outboard load cases; it can be seen that there is a significant difference between the various load cases, particularly between the local flexural axis and the global cases.

On a real aircraft wing there is usually a pitching moment contribution ($C_{M0} \neq 0$) due to the camber of the wing surface. However, the same methodology as above can be used to determine the various flexural axis positions as the aerodynamic loads that are applied to an aircraft lifting surface act normal to the wing surface and these can be resolve to lift, drag and pitching moment, which in turn can be resolved to forces acting at the leading and trailing edges.

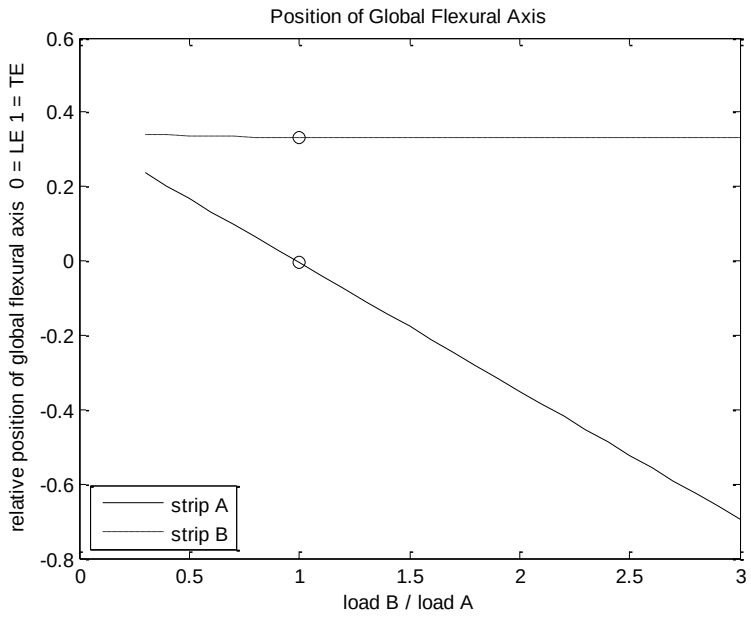

Figure 4. Global flexural axis position for a varying applied load ratio on the 2-strip swept wing

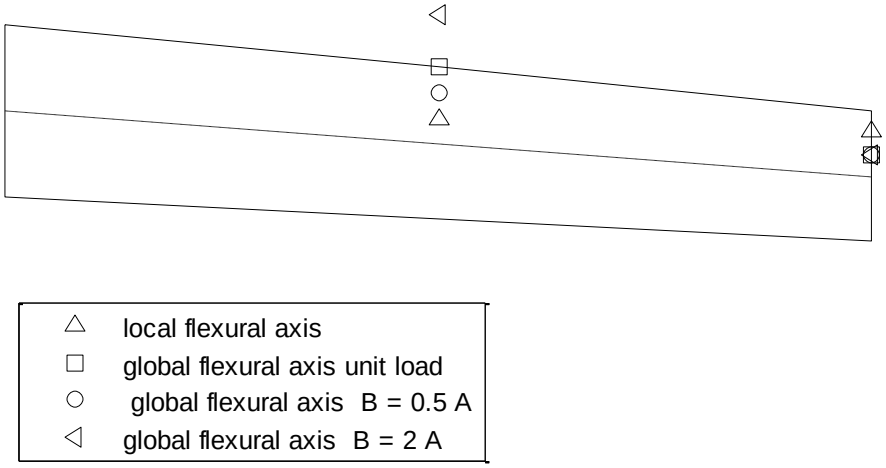

Figure 5. Position of shear center, local and global flexural axes on the 2-strip swept wing

B. Flexural Axes of an Aluminum Wing Box

Now consider the representative aft-swept, tapered, symmetric aluminum wing-box FE model shown in Figure 6, containing conventional spars, ribs, skins and stringers formed from an outer wing-box (OWB) and half a center wing box (CWB) with dimensions described in Table 2. The wing box sweep, span, height and chord are representative of the NASA Common Research Model[14], although the wing box considered here is straight (constant sweep and taper), it has no dihedral or twist, and panels are flat for simplicity. The skins, spars and ribs were modeled with a uniform panel thickness of 5mm and uniform section stringers and the CWB is fully constrained at its root. The FE model was analyzed using NASTRAN v2012.1 and included 12000 shell elements and 4000 stringer beam elements.

Table 2. Aluminum wing box parameters

CWB Semi-span	**CWB Chord**	**CWB Height**	**Stringer Pitch**	**OWB Rib pitch**
3.05m	7.04m	1.04m	0.40m	1.36m
OWB span	**OWB Tip Chord**	**OWB Tip Height**	**OWB Front Spar Sweep Angle**	
26.19m	1.66m	0.16m	35.77deg	

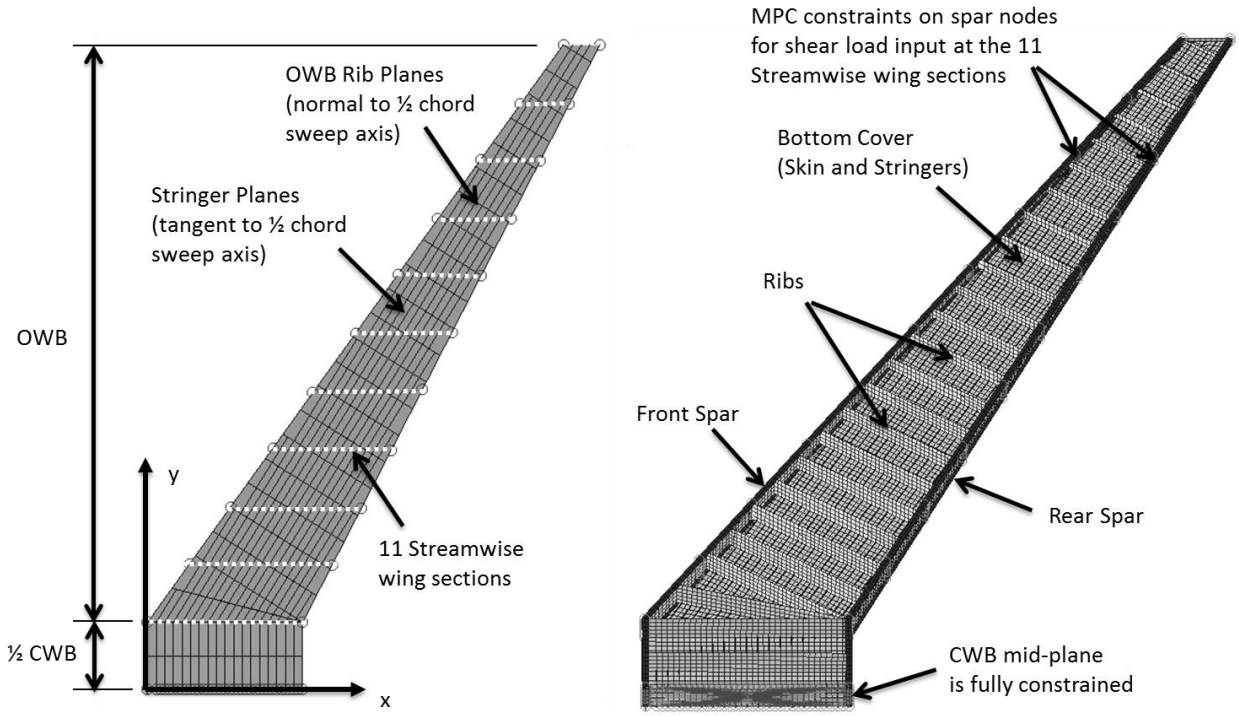

Figure 6. Aluminum wing box model

1. Flexural Axis Computation

The flexibility matrix for this wingbox was determined by applying unit loads at 11 pairs of leading edge and trailing edge positions (on 11 streamwise wing sections). The approaches described in the previous section, adjusted to include the larger number of loading pairs, were then used to determine the local and global flexural axes for three possible types of different distributed loads: uniform, triangular and elliptical. Although the distributed loads, and hence the flexural axis position, would vary at different points in the flight envelope, only computation of a few typical distributions is required as the methodology requires only the ratio of the distributed loads to be defined. Such an analysis requires much less computation compared to determining the static wing deflection at all points of the flight envelope. Figure 7 compares the results obtained for each case and it can be seen that the local flexural axis is positioned at the elastic axis in-board but then moves forward of the leading edge at around the mid span. The three continuous loading cases lead to different results for the global flexural axis, and they are all forward of the leading

edge at the root, and then move onto the wing planform towards the wing tip. Since the triangular and elliptic load distributions tend to zero at the tip of the wing, the corresponding global flexural axes are only plotted over the inboard 10 streamwise wing sections.

Note that the kink in the global flexural axes at wing root (section #2 in Figure 7) is a feature of the load transfer between the swept OWB and unswept CWB. Due to the change in sweep angle, the rear spar tends to be stiffer and more highly loaded than the front spar at the root of the OWB[15], such that the OWB effectively twists about a point aft of the elastic axis at the root of the OWB. This locally increases the moment arm of a shear load applied towards the leading edge of the wing and causes the global flexural axis to move aft at wing section #2. The global flexural axis moves forward significantly again at section #1, to compensate for the twist induced by the OWB loads transferred mainly through the rear spar; this behavior of the flexural axis position at the root is a characteristic of the imposed boundary conditions.

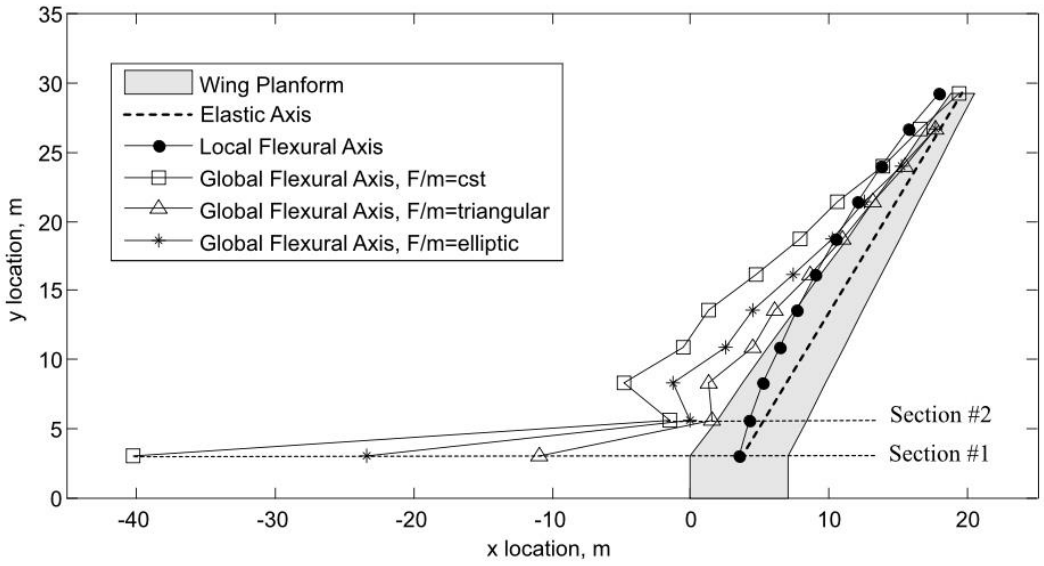

Figure 7. Local and global flexural axes and elastic axis for the aluminum wing box

C. Flexural Axes of a Tailored Composite Wing

As a further example, we consider the simple unswept and untapered cantilevered plate wing previously used for studies into the application of tow-steered, variable stiffness composites[16]. Two different wing composite laminates are considered: a unidirectional (UD) ply laminate (constant fiber angle in each ply) and a variable-angle-tow (VAT) ply laminate (continuous fiber angle variations in the outer plies as function of the spanwise location). Both are 8-ply symmetric laminates with an inner ply stack of $[-45/+45]_s$ and outer ply fiber angles shown in Figure 8. Both laminates were optimized such as to minimize the wing root forces due to different applied (1-cosine) discrete gust loads. Since the laminates are not balanced, the bending and torsion deformations are coupled.

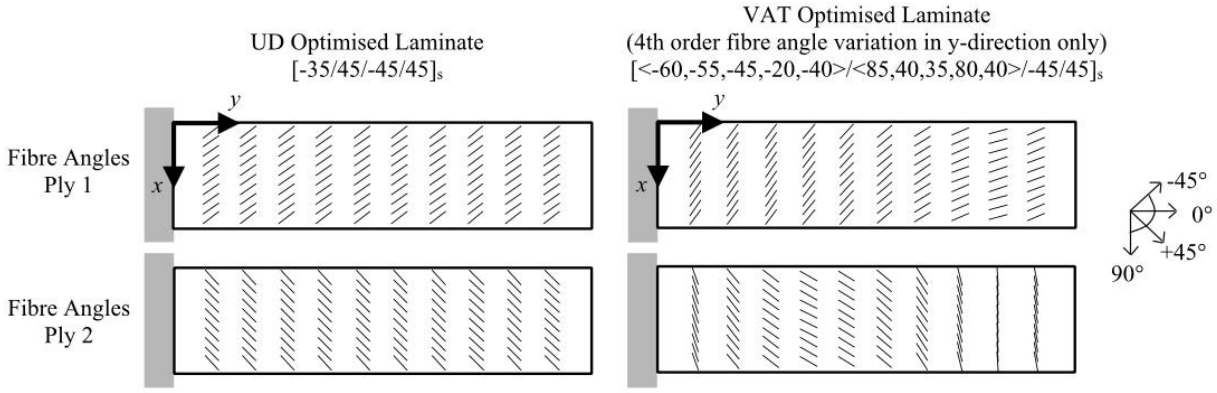

Figure 8. Optimized UD and VAT composite layups for the cantilevered plate wing[14]

1. Flexural Axis Computation

The flexibility matrix was determined as before by applying unit loads at 16 pairs of leading edge (x=0) and trailing edge (x= 76.2mm) positions and the local and global flexural axes determined for three different distributed loads: uniform, triangular and elliptical. It can be seen that the global and local flexural axes differ significantly. For the UD case, shown in Figure 9, the local flexural axis moves forward of the leading edge beyond the mid-span, whereas, the global flexural axes all have the opposite gradient and are placed, on the wing, at spanwise positions close to the wingtip. The global flexural axes have similar trends for the different load distributions, with bigger differences at the root. It should be noted that all flexural axes are straight lines in this case.

Figure 10 shows the same results for the VAT test case, where the local flexural axis is again very different from the global flexural axes, the former moving forwards with increasing spanwise position, whereas the three global cases all demonstrate the same "s" type shape. All of the distributed load cases show the same extreme forward position of the global flexural axis towards the wing root, similar to the axes found for the aft-swept aluminum wing box in the previous section.

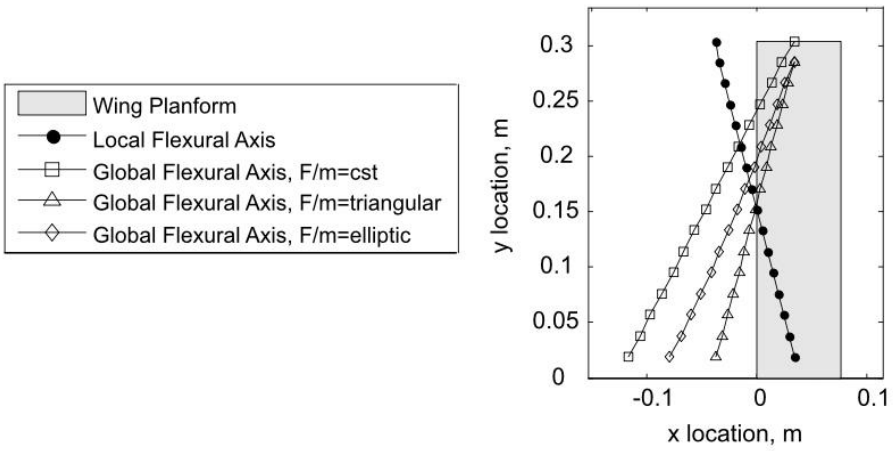

Figure 9. Local and global flexural axes for the optimized UD laminate wing

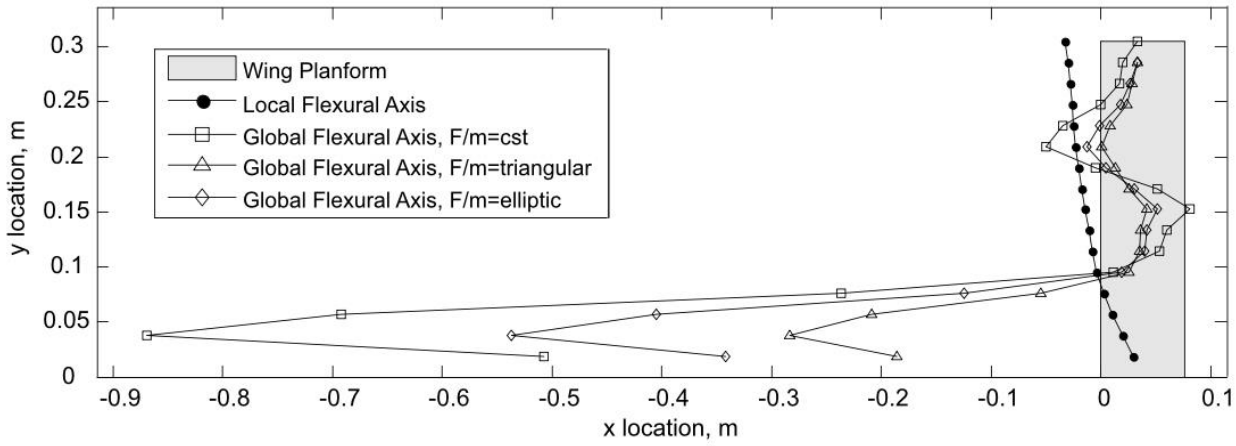

Figure 10. Local and global flexural axes for the optimized VAT laminate wing

2. Analytical Computation of Composite Wing Flexural Axes

For this simple wing, the flexural axes positions can be verified analytically. Classical Laminate Theory[17] provides analytical relations between the local bending and twisting moments per unit length and mid-plane curvatures for a composite laminate. For a chordwise rigid wing (k_x=0), with no constraint on the chordwise moment, it can be shown that the wing spanwise bending curvature (w'') and twist rate (θ') are related to the bending moment (M) and torque (T) by

$$\begin{bmatrix} M \\ T \end{bmatrix} = c \begin{bmatrix} D_{22} & 2D_{26} \\ 2D_{26} & 4D_{66} \end{bmatrix} \begin{bmatrix} w'' \\ \theta' \end{bmatrix} \tag{9}$$

and solving for the twist rate gives

$$\theta' = \frac{\overline{T}\,\overline{D}}{4c}$$

with (10)

$$\overline{T} = T - \frac{2D_{26}}{D_{22}} M \quad ; \quad \overline{D} = \frac{1}{D_{66} - {D_{26}}^2 / D_{22}}$$

where $\overline{T}$ and $\overline{D}$ are modified torque and reduced stiffness terms, respectively. Note that the reduced torque $\overline{T}$ can be larger or smaller than the applied torque T, depending on the sign of the applied moment and the sign of the stiffness coupling term D_{26}; however, the stiffness D always reduces

The location of the local flexural axis (or flexural center) x_L at a certain spanwise location y_p is determined by setting the chordwise section twist angle $\theta(y_p)$ due to a shear load P applied at (y_p , x_L) to zero (for $\theta(0) = 0$). By substituting the bending moment and torsion distributions due to P into equation (10) and then integrating this equation, we find

$$\left.\begin{array}{c} \theta(y_p) = \int_0^{y_p} \theta' dy \; = 0 \\ T = P\left(x_L(y_p) - \frac{c}{2}\right) \\ M = P(y_p - y) \end{array}\right\} \Rightarrow \quad x_L(y_p) = \frac{2\int_0^{y_p} \frac{\overline{D}\, D_{26}}{D_{22}} (y_p - y) dy}{\int_0^{y_p} \overline{D}\, dy} + \frac{c}{2} \tag{11}$$

where c is the local streamwise wing section chord-length.

Knowing the spanwise distributions of the stiffness parameters D_{22}, D_{26} and D_{66}, the local flexural axis position $x_L(y_p)$ can then be calculated at any spanwise location y_p. The prediction can be improved by including the wing root warping constraint[6] in equation (10), such that $\theta'(0) = 0$ is satisfied, thus

$$x_L(y_p) = \frac{2\displaystyle\int_0^{y_p} \frac{\overline{D}\,D_{26}}{D_{22}}(y_p - y)\left(1 - \frac{\cosh(\mu(y_p - y))}{\cosh(\mu\, y_p)}\right) dy}{\displaystyle\int_0^{y_p} \overline{D}\left(1 - \frac{\cosh(\mu(y_p - y))}{\cosh(\mu\, y_p)}\right) dy} + \frac{c}{2} \tag{12}$$

where μ is a laminate dependent warping constant. For the wing examples presented here, μ was calibrated to provide a good correlation between the analytical predictions and the flexibility matrix predictions. For a more rigorous approach, μ could be determined as a function of the laminate stiffness properties and plate dimensions[18]; however, this is beyond the scope of this current work.

The location of the global flexural axis $x_G(y)$ can be determined for a specific applied load case by simply setting the twist rate to zero in equation (10). For instance, a uniform constant load distribution $P(y) = P$ on the wing of span s, this leads to

$$\left.\begin{aligned} T &= -P\int_s^y x_G(y) - \frac{c}{2}\, dy \\ M &= P\,(s-y)^2/2 \end{aligned}\right\} \Rightarrow \quad x_G(y) = 2\frac{D_{26}}{D_{22}}(s-y) - \frac{\partial\,(D_{26}/D_{22})}{\partial y}(s-y)^2 + \frac{c}{2} \tag{13}$$

For the UD laminate, since $\partial\,(D_{26}/D_{22})/\partial y = 0$, equation (13) shows that the global flexural axis is a straight line from $x = 2s\,(D_{26}/D_{22}) + c/2$ at the root to $x = c/2$ at the tip of the wing. Similar results can be obtained for different lift distributions.

The flexural axes calculated using the flexibility matrix approach and the analytical expressions are compared in Figure 11 and Figure 12. The two predictions correlate relatively well, although some discrepancies are observed, which originate mainly in the limited number of mode shapes assumed by the Rayleigh-Ritz method used to calculate the plate flexibility matrix. As the number of mode shapes and reference points along the span is increased, the numerical results tend towards the analytical predictions.

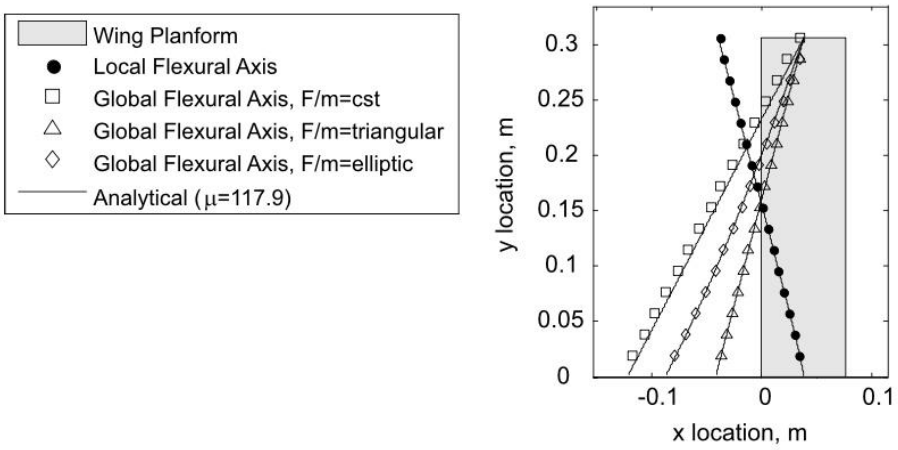

Figure 11. Comparison of numerical and analytical flexural axis predictions for the UD laminate

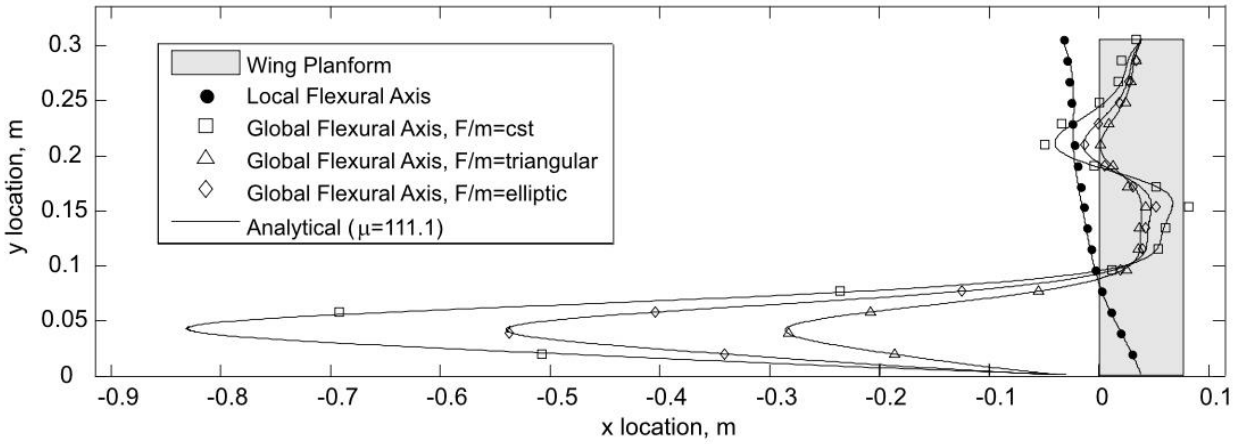

Figure 12. Comparison of numerical and analytical flexural axis predictions for the VAT laminate

IV. Sensitivity Analysis of Flexural Axes Prediction

It is of interest to determine the sensitivities of the flexural axes, calculated in Section III, with respect to errors and uncertainty. These are likely to occur in the flexibility matrix computation due to either inaccuracies in the structural and aerodynamic computational modeling, or measurement errors when the flexural axes have been determined experimentally. The sensitivity in the estimated flexural axes positions is computed using Monte-Carlo simulations.

A. Sensitivity Analysis of Flexural Axes Position for Aluminum Wing- Numerical Results

A Monte Carlo sensitivity analysis was performed to determine the effect of variations in the flexibility matrix on the flexural axes locations. A uniform random error of up to ±1% was applied to the flexibility matrix terms of a million samples (maintaining matrix symmetry) and the probability distributions of the resulting flexural axes locations errors extracted for the uniform load, triangular and elliptical load cases. Normal distributions were typically for all of the global flexural axis variations whereas there was some skewness in the local flexural axis distributions towards the wing tip.

The error sensitivity of the flexural axes can be then be visualized by plotting the 95% confidence range of the flexural axis at each spanwise locations, as shown in Figure 13. These results show that the global flexural axes locations are highly sensitive to errors in the flexibility matrix, as small input errors of ±1% can induce variations of several span lengths in the predicted streamwise position of the global flexural axis. The variations for the constant loading case are much greater than the other two global loading distributions. Conversely, the local flexural axis is significantly less sensitive to errors than any of the global flexural axes calculations.

Similar findings were obtained from the sensitivity analysis of the composite wing box test cases and are therefore not shown for reasons of conciseness.

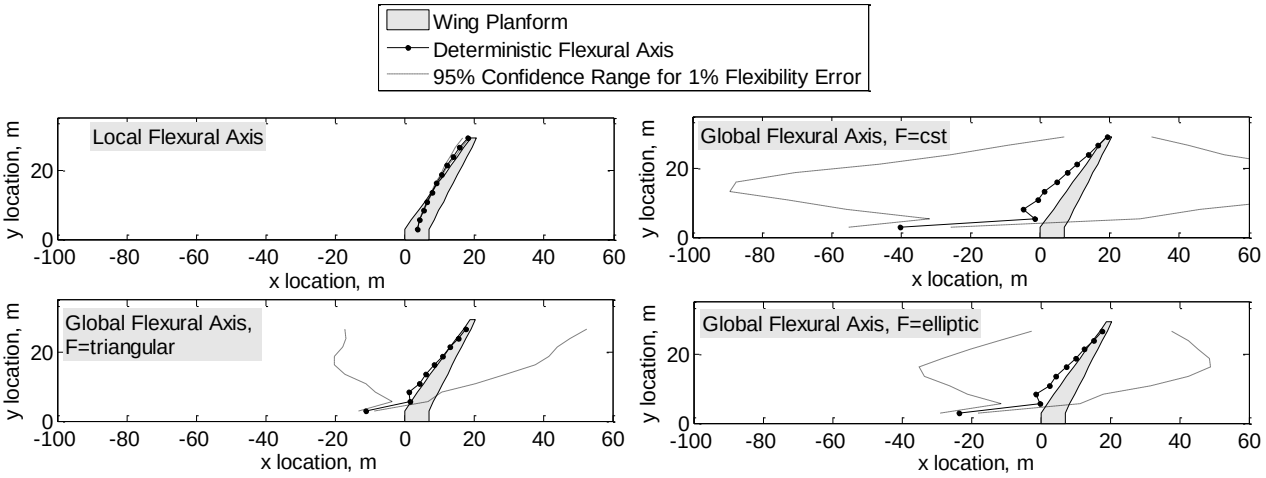

Figure 13. 95% Confidence bounds for local and global flexural axes

V. Conclusions

The definitions of the axis on a general swept, non-uniform, non-homogenous wing about which there is no bending / torsion coupling have been reviewed. A generalization of these definitions is made, with an emphasis on differences between whether a local streamwise section or the entire wing is considered. Through the use of a flexibility matrix approach, it has been demonstrated that the loading case must be considered in order to be able to accurately determine the flexural axis of a typical wing structure and how this can be used to interpret the aeroelastic behavior of the wing. The approach was demonstrated using three models: a simple swept wing, an aluminum wing box, and a tow-steered composite plate wing showing significant differences between the local and global flexural axes. Finally, the sensitivity of the flexural axis was considered and it was shown that a global flexural axis prediction is much more sensitive to modeling or measurement errors than that of the local flexural axis.

VI. Acknowledgements

The authors are grateful for the support of the EPSRC, Airbus Operations Ltd and the Royal Academy of Engineering.

VII. References

[1] Bisplinghoff, R. L., Ashley, H., and Halfman, R. L. *Aeroelasticity*. New York: Dover Publications, 1996.

[2] Wright, J. R., and Cooper, J. E. *Introduction to Aircraft Aeroelasticity and Loads*: Wiley, 2007.

[3] Weisshaar, T. A. "Aeroelastic tailoring - Creative Uses of Unusual Materials," *28th Structures, Structural Dynamics and Materials Conference*. American Institute of Aeronautics and Astronautics, 1987.

[4] Wagg D., Bond I., Weaver P.M., and Friswell M. *Adaptive Structures: Engineering Applications*. Wiley 2007

[5] R. Tatham, B. A., "Shear Centre, Flexural Centre and Flexural Axis: An Attempt to Clear up Current Confusion and Provide Definitions Differentiating Between the Three Terms," *Aircraft Engineering and Aerospace Technology* Vol. 23, No. 7, 1951, pp. 209 - 210

[6] Megson, T. H. G. *Aircraft Structures for Engineering Students*. London New York: 4th Elsevier, 2007.

[7] Young, W. C., Budynas, R. G., and Roark, R. J. *Roark's Formulas for Stress and Strain*. New York: McGraw-Hill, 2002.

[8] Niles, A. S., and Newell, J. S. *Airplane Structures*. New York,: Wiley, 1954.

[9] Peery, D. J. *Aircraft Structures*. New York,: McGraw-Hill, 1950.

[10] Kuhn, P. *Remarks on the Elastic Axis of Shell Wings*: National Advisory Committee for Aeronautics. Langley Aeronautical Lab.; Langley Field, VA, United States, 1936, NACA-TN-562.

[11] Fung, Y. C., *An Introduction to the Theory of Aeroelasticity*. New York: Dover Publications, 1993.

[12] Yu, W., Volovoi, V. V., Hodges, D. H., and Hong, X. "Validation of the Variational Asymptotic Beam Sectional Analysis," *AIAA Journal* Vol. 40, No. 10, 2002, pp. 2105-2112

[13] Rehfield, R.W., and Atilgan, A.R., "Shear Center and Elastic Axis and their Usefulness for Composite Thin-Walled Beams". *Proceedings of the American Society for Composites, Fourth Technical Conference*. Blacksburg, Virginia, 1989 pp. 179-188.

[14] Vassberg, J., DeHaan, M., Rivers, S., and Wahls, R. "Development of a Common Research Model for Applied CFD Validation Studies," *26th AIAA Applied Aerodynamics Conference*. Honolulu, Hawaii. 2008. AIAA 2008-6919

[15] Niu, M.C.Y. *Airframe Structural Design - Practical Design Information and Data on Aircraft Structures*, 2nd ed., Conmilit Press Ltd.,, Hong Kong, 1999.

[16] Stodieck, O., Cooper, J. E., Weaver, P., and Kealy, P. "Optimisation of Tow-Steered Composite Wing Laminates for Aeroelastic Tailoring," *55th AIAA/ASMe/ASCE/AHS/SC Structures, Structural Dynamics, and Materials Conference*. American Institute of Aeronautics and Astronautics, 2014.

[17] Jones, R. *Mechanics of Composite Materials*: CRC, 1998.

[18] Hodges, D. H., *Nonlinear Composite Beam Theory*. Reston, Va.: American Institute of Aeronautics and Astronautics, 2006.